Dynamical screening in the cooling theory of high-density electron-hole plasmas

J. H. Collet
Département de Physique, Centre National de la Recherche Scientifique–Institut National des Sciences Appliquées, Avenue de Rangueil, 31077 Toulouse, France
(Received 28 March 1988; revised manuscript received 25 July 1988)

We calculate the LO-phonon emission rate and the energy transfer from carriers to the lattice using a dynamical screening of the electron-phonon interactions in the random-phase approximation. We consider a three-dimensional homogeneous plasma. Because of the computational difficulties encountered when screening dynamically, we restrict our study to the partly thermalized regime. We analyze particularly the LO-phonon emission rates by electrons and holes at room temperature and at liquid-helium temperature. Electrons are more sensitive than holes to dynamical effects. Contrary to the results deduced in the static approximation, we conclude from our general study that the screening of the LO-phonon emission has no significant effect on the cooling up to the density ρ_c, corresponding to the resonance of LO phonons with plasmons, determined by the equation $\hbar\omega_{\mathrm{LO}} \simeq \hbar\omega_{\mathrm{pl}}(\rho_c)$. Here, $\hbar\omega_{\mathrm{LO}}$ and $\hbar\omega_{\mathrm{pl}}(\rho_c)$ are, respectively, the LO-phonon energy and the plasmon energy. In GaAs, $\rho_c \simeq (5-7)\times 10^{17}$ cm^{-3}. At plasma densities higher than ρ_c, the dynamical screening tends to the static one, but the effect depends quantitatively on the plasma temperature.

I. INTRODUCTION

Dense, electron-hole plasmas have been generated for many years in direct-gap semiconductors through absorption, first, of nanosecond optical pulses[1,2] and thereafter of picosecond and even subpicosecond pulses. Such experiments have often been carried out for investigating the electron-hole plasma dynamics. We quote here, in a nonexhaustive list, several time-resolved picosecond-luminescence studies on GaAs (Refs. 3–8) which investigated the relaxation dynamics of the carrier kinetic energy as well as the kinetics of the plasma density. Time-resolved transmission experiments, for photons with an energy close to the band-gap one, are also of great interest for studying the plasma dynamics as demonstrated in previous works.[9–11] The internal plasma thermalization (i.e., the transition from nonthermalized carrier distributions to Fermi-Dirac–like distributions) was also studied in Ref. 12 using the generation of a cold and degenerate plasma with subpicosecond pulses. Simultaneously, several theoretical models have been developed to account for the internal plasma thermalization and also for the transfer of the plasma energy to the lattice, starting from general transport equations without, as much as possible, adjustable parameters.[13–25]

In the present study, we wish to discuss briefly the energy transfers from the carriers to the lattice, especially considering the dynamical screening of the electron-phonon interactions in a dense plasma.[13,14]

We shall restrict our study to a three-dimensional homogeneous plasma. The cooling of dense plasmas in quantum wells is therefore not discussed. For more information on this subject, see, for instance, Refs. 15 and 16. Because of the computational difficulties encountered when screening dynamically, we restrict our analysis to the partly thermalized regime. It is well known that, under excitation by subpicosecond pulses, carrier distributions are not generally thermalized during the first picosecond. The plasma is athermal.[12,17–19] Fortunately, very often, typically one picosecond after the excitation (in the case of subpicosecond pulses), a partly thermalized regime takes place: electrons and holes are thermalized at two different temperatures. We shall restrict our analysis to this regime. The description of the carrier distributions becomes greatly simplified with respect to the athermal case because only three parameters are necessary to determine the two distributions; namely, the temperatures of the two types of carriers and the plasma density. Under these relatively simple conditions, one may attempt to include the dynamical screening of the different interactions in the description of the plasma dynamics. In the current literature,[13,14,20–24] electron-phonon and electron-hole interactions are generally not screened or screened statically without any discussion, except in the work of Yoffa,[25] which was restricted to nondegenerate plasmas. The static approximation holds obviously as long as the energy ΔE exchanged in the interaction processes is small compared to the plasmon energy $\hbar\omega_{\mathrm{pl}}$;[19] for instance, in the case of emission or absorption of acoustical phonons and often for the electron-hole interactions. The discussion of screening of the electron-hole collisions is reported in the Appendix. The energy condition $\Delta E \ll \hbar\omega_{\mathrm{pl}}$ is usually not fulfilled for the emission of LO phonons. Using a static dielectric function to screen this process is therefore *a priori* questionable. As the emission of LO phonons [via polar-optical (PO) interaction] is often the dominant plasma-energy-loss process, it is of importance to clarify the impact of dynamically screening the PO interaction, especially for the plasma densities leading to the resonance of LO phonons with plasmons (in GaAs, around the plasma density $\rho \simeq 7\times 10^{17}$ cm^{-3}). In this case, the emission of

short-wave-vector LO phonons can be strongly enhanced. The understanding of recent experiments also demands an accurate calculation of the PO screening. For instance, plasma heating experiments in GaAs (for $\rho \leq 4\times 10^{17}$ cm^{-3})[26] which include a negligible screening of the polar-optical coupling and numerous subpicosecond experiments which generate electrons of high kinetic energy in the conduction band. The dynamics of the hot carriers on a time scale of the order of 1–2 ps involves the dominant emission of short-wave-vector LO phonons and requires a dynamical treatment of screening. We shall show in Sec. III that the use of the static screening in thermalized conditions may underestimate the plasma-energy-loss rate by 1 order of magnitude with respect to the full dynamical treatment.

As we focus our attention on screening, we shall not consider a nonequilibrium population of LO phonons. This approach is justified in heating experiments[26,27] or in the energy-relaxation studies of athermal carriers in the subpicosecond or the picosecond regime. On time scales of several tens of picoseconds, nonequilibrium LO-phonon distributions appear very quickly when generating hot and dense electron-hole plasmas. This situation is extensively discussed in Ref. 20. It is concluded that an accurate screening theory of the electron–LO-phonon interaction is not essential provided that the plasma cooling is accompanied by a quick saturation of the LO-phonon modes strongly coupled to electrons and holes. The great majority of the experimental investigations on plasma cooling have been carried under these conditions of thermalized plasmas and low temperatures. Investigations at high temperature[5] (especially at room temperature) are also of great interest due to their real link with the physics of ultrafast devices, although it becomes more difficult to significantly disturb the LO-phonon distribution because the LO-phonon occupation $n_{\rm LO}$ at equilibrium is already high [for example, in GaAs, $n_{\rm LO}(T=300$ K$)=0.36$], and also because the LO-phonon lifetime $\tau_{\rm LO}$ is typically three times shorter than at low temperature. In GaAs, the thermalization time of the perturbed LO-phonon distribution is of the order of 2–4 ps at room temperature.[28]

In the following, we shall compute separately the LO-phonon emission rates by electrons and holes to stress the importance of dynamically screening the conduction-band electrons, particularly if a temperature difference appears between the carriers (i.e., $T_e > T_h$). It is generally assumed, in the analysis of experimental works on high-density-plasma cooling, that electrons and holes are thermalized at the same temperature. Under this assumption, the high-energy tail of the luminescence spectra enables determination of the plasma temperature. This assumption is, however, not obvious and has already been questioned (see, for example, Ref.21). If the electron and hole temperatures are different, luminescence experiments determine in effective temperature $T_{\rm eff}$ very close to that of the electrons T_e, because the electron mass is generally much smaller than the hole mass. A straightforward calculation shows that, in a free-particle model, the high-energy tail of the luminescence spectra decreases as $\exp(-h\nu/k_B T_{\rm eff})$ with $T_{\rm eff}$ defined by

$$\frac{m_e+m_h}{T_{\rm eff}}=\frac{m_h}{T_e}+\frac{m_e}{T_h}\ ,$$

where m_e (m_h) is the electron (hole) mass and T_h is the hole temperature. For example, in GaAs, even if the temperature difference is important, say $T_e/T_h=2$, one deduces that $T_{\rm eff}\simeq 0.9T_e$, which proves that this is the electron temperature which is really accessible experimentally. As a result, it should be necessary to investigate experimentally the temperature kinetics of holes which cannot be deduced unambiguously from the above formula. New experiments on hole dynamics are in progress.[29]

II. THEORETICAL BACKGROUND

In the following, we wish to calculate the transfer of energy from the photogenerated plasma to the lattice. This implies, *a priori*, that we must separate the electronic degrees of freedom from the lattice, in order to define unambiguously both the energy levels E_i of the photogenerated-plasma states $|\Psi_i\rangle$ and the electronic energy transferred to the lattice. The plasma states $|\Psi_i\rangle$ are many-body electron states, fully including the electron-electron interactions. Energy is transferred by transition of the photoexcited plasma between the states $|\Psi_i\rangle$ (Ref. 30) due to the usual coupling Hamiltonian $H_{\rm in}=\sum_\lambda V_\lambda(q)\rho_q^\lambda(b_q+b_{-q}^\dagger)$. λ is an electron-band index, ρ_q^λ is the Fourier transform of the carrier density operator $\rho(r)=\sum_\lambda \rho_q^\lambda e^{iqr}$, and $b_q^\dagger$ (b_q) is the creation (destruction) operator of a phonon of wave vector q. Interband phonon-assisted transitions have been omitted. We follow, at the beginning, Kogan's approach,[31] which we extend to a many-band plasma. The phonon-emission rate $dn_{\rm LO}(q)/dt|_+$ and phonon-absorption rate $dn_{\rm LO}(q)/dt|_-$ read

$$\left.\frac{dn_{\rm LO}(q)}{dt}\right|_\pm=\frac{2\pi}{\hbar}\sum_\lambda |V_\lambda^{\rm LO}(q)|^2[\tfrac{1}{2}\pm\tfrac{1}{2}+n_{\rm LO}(q)]\times\sum_{i,f}p_i^{T_p}(t)|\langle\Psi_f|\rho_{-q}^\lambda|\Psi_i\rangle|^2\times\delta(E_i-E_f\mp\hbar\omega)\ .$$

Here, $p_i^{T_p}(t)$ is the density matrix of the photoexcited plasma at the temperature T_p. If phonons are thermalized at temperature T, we use the notation $n_{\rm LO}^T$ instead of $n_{\rm LO}(q)$. After some algebra, one deduces the net emission rate [i.e., the difference between $dn_{\rm LO}(q)/dt|_+$ and $dn_{\rm LO}(q)/dt|_-$], which reads

$$\frac{dn_{\rm LO}(q)}{dt}=\frac{2}{\hbar}\sum_\lambda |V_\lambda^{\rm LO}(q)|^2[n_{\rm LO}(q)-n_{\rm LO}^{T_p}]\times{\rm Im}[\Pi_\lambda(q,\omega(q))] \quad (1)$$

with

$$\Pi_\lambda(q,\omega(q))=\frac{1}{i\hbar}\int_{-\infty}^0\langle[\rho_q^\lambda(0),\rho_{-q}^\lambda(\tau)]\rangle e^{i\omega\tau}d\tau\ . \quad (2)$$

Here, $\langle\ \rangle$ denotes the full statistical average of any electronic observable quantity X: $\langle X\rangle={\rm Tr}(\rho X)$. Π_λ is the

well-known polarization diagram. Im(Π) is the imaginary part of Π. Using a diagrammatic expansion in a series of *irreducible* polarization kernels $\Pi_\lambda^{\rm ir}(q,\omega)$,[32] one deduces

$$\Pi_\lambda(q,\omega)=\Pi_\lambda^{\rm ir}(q,\omega)+\frac{[\Pi_\lambda^{\rm ir}(q,\omega)]^2V_0(q)}{1-\sum_\nu \Pi_\nu^{\rm ir}(q,\omega)V_0(q)} . \quad (3)$$

The denominator is the plasma dielectric function $\epsilon(q,\omega)$ and $V_0(q)$ is the Fourier transform of the Coulomb potential. We get, after some algebra,

$$\mathrm{Im}(\Pi_\lambda)=\frac{\mathrm{Im}(\Pi_\lambda^{\rm ir})}{|\epsilon(q,\omega)|^2}\left|1-\sum_{\nu\neq\lambda}\Pi_\nu^{\rm ir}\right|^2 + \sum_{\nu\neq\lambda}\mathrm{Im}(\Pi_\nu^{\rm ir})\left|\frac{\Pi_\lambda^{\rm ir}}{\epsilon(q,\omega)}\right|^2 . \quad (4)$$

In a two-component electron-hole plasma (so that $m_h \gg m_c$) we use the following simple approximation:[33] $\mathrm{Im}(\Pi_\lambda)\simeq\mathrm{Im}(\Pi_\lambda^{\rm ir})/|\epsilon(q,\omega)|^2$. We obtain from Eq. (1) the basic formula describing the LO-phonon emission rate by the band λ in a many-band system:

$$\left.\frac{dn_{\rm LO}(q)}{dt}\right|_\lambda=\frac{2}{\hbar}\left|\frac{V_\lambda^{\rm LO}(q)}{\epsilon(q,\omega_{\rm LO})}\right|^2[n_{\rm LO}(q)-n_{\rm LO}^{T_p}] \times\mathrm{Im}[\Pi_\lambda^{\rm ir}(q,\omega_{\rm LO})] . \quad (5)$$

This expression holds for any density of the photogenerated plasma. Starting from the full many-electron states, it has been therefore concluded that the plasma polarization effects at high density are taken into account through the plasma dielectric function which renormalizes the polar interaction. We stress that we did not have to split the plasma energy into an elementary-excitation energy and a collective-mode energy, which is very artificial. The concept of plasmon emission by the single particles (and also to some extent the emission of mixed plasmon-phonon modes) is irrelevant and cannot be considered as an energy-loss process of the plasma. The phonon-emission rate for each band reads

$$\left.\frac{dn_{\rm LO}(q)}{dt}\right|_\lambda=-\frac{2}{\hbar}M_\lambda\left[1-\frac{\epsilon_\infty}{\epsilon_0}\right]\omega_{\rm LO}[n_{\rm LO}(q)-n_{\rm LO}^{T_p}] \times\frac{\epsilon_2^\lambda(q,\omega_{\rm LO})}{\epsilon_1^2(q,\omega_{\rm LO})+\epsilon_2^2(q,\omega_{\rm LO})} . \quad (6)$$

For each band λ, the average energy-loss rate per particle $(1/\rho)\,(d\langle E_\lambda\rangle/dt)|_{\rm LO}$ is related to the phonon-emission rate by

$$\left.\frac{1}{\rho}\frac{d\langle E_\lambda\rangle}{dt}\right|_{\rm LO}=-\frac{1}{\pi^2\rho}\int_0^{+\infty}\hbar\omega_{\rm LO}q^2dq\left.\frac{dn_{\rm LO}(q)}{dt}\right|_\lambda . \quad (7)$$

M_λ is the correction factor of the Frölich interaction of LO phonons with the band λ.[34] As we do not consider any significant perturbation of the LO-phonon distribution with respect to its equilibrium value at the lattice temperature T_l, we set $n_{\rm LO}(q)=n_{\rm LO}^{T_l}$ in the right-hand side of Eq. (6). The dielectric function is calculated in the random-phase approximation (RPA). The real and imaginary parts read, after some algebra,

$$\epsilon_1(q,\omega)=1-\sum_\lambda\frac{2m_\lambda e^2}{\epsilon_\infty\hbar^2\pi q^3} \times\int_0^{+\infty}kf_\lambda(k)\left[\ln\left|\frac{k+K_0^\lambda}{k-K_+^\lambda}\right| +\ln\left|\frac{k+K_-^\lambda}{k-K_-^\lambda}\right|\right]dk ,$$

$$\epsilon_2(q,\omega)=\sum_\lambda\epsilon_2^\lambda(q,\omega)=\sum_\lambda\frac{2m_\lambda e^2}{\epsilon_\infty\hbar^2q^3}\int_{K_-^\lambda}^{K_+^\lambda}Kf_\lambda(K)dK$$

with $K_\pm^\lambda=q/2\pm m_\lambda\omega/\hbar q$.

III. NUMERICAL RESULTS: PHONON-EMISSION RATE

We specialized our numerical study to GaAs. We used the material parameters listed in Ref. 13. The way dynamical screening influences the carrier-energy relaxation might seem somewhat mysterious in displaying directly the energy-loss rate $(1/\rho)(\langle dE_\lambda\rangle/dt)_{\rm LO}$ reported in Figs. (3–6). For clarity, we report first, in Fig. 1(a), the computation of the quantity $1/|\epsilon(q,\omega_{\rm LO})|^2$ as a function of the phonon wave vector q. This quantity is re-

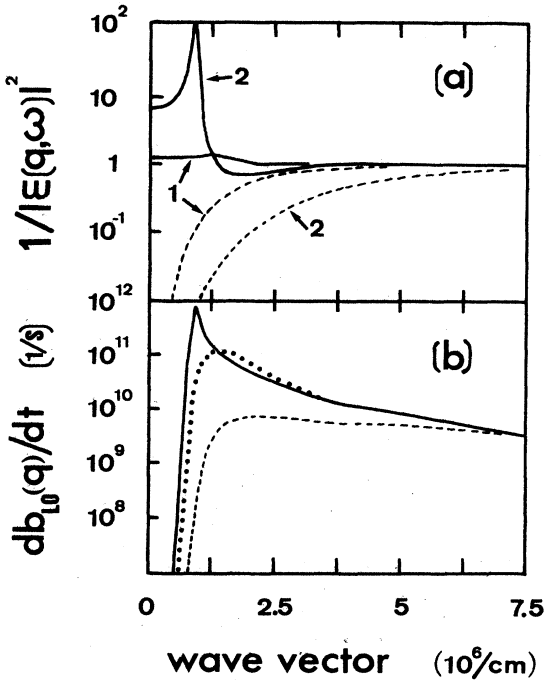

FIG. 1. Plasma temperature, 100 K; lattice temperature, 4 K. (a) Renormalization factor of the Fröhlich interaction. Curves 1: density $\rho=5\times10^{16}$ cm^{-3}. Curves 2: density $\rho=4\times10^{17}$ cm^{-3}. Solid lines, full RPA; dashed lines, static screening. (b) LO-phonon-emission rate. Solid lines, full RPA; dashed lines, static screening; dotted line, no screening.

sponsible for the enhancement or the damping of the emission probability of LO phonons of wave vector q. In the low-density range, typically for $\rho \simeq 5\times 10^{16}$ cm^{-3}, the LO-phonon energy $\hbar\omega_{LO}$ is much larger than that of the plasmon, $\hbar\omega_{pl}$. As a result, in the full RPA calculation [Fig. 1(a), solid line 1], $1/|\epsilon|^2$ always remains very close to 1. In other words, there is no significant screening effect. The static approximation of $1/|\epsilon|^2$ [Fig. 1(a), dashed line], which reads

$$\frac{1}{|\epsilon|^2}=\frac{1}{|q^2+q_{DH}^2|^2},$$

is obviously in error. Here q_{DH} is the Debye-Hückel wave vector. At the second density $\rho=4\times 10^{17}$ cm^{-3}, a strong resonance appears around $q=10^{-6}$ cm^{-1} in the full RPA calculation [Fig. 1(a), solid line 2]. This is a general behavior of $1/|\epsilon|^2$ when the density is close to $\rho_c=(4-7)\times 10^{17}$ cm^{-3} in GaAs. This enhancement appears when the following resonance condition of the optical plasmon with the LO phonon is fulfilled:

$$\hbar\omega_{pl}(\rho_c)=\hbar\omega_{LO}$$

with

$$\hbar\omega_{pl}(\rho_c)^2=4\pi\rho_c e^2\left[\frac{1}{m_c}+\frac{1}{m_v}\right].$$

Now, the quantity of interest, to determine the total phonon-emission rate dn_{LO}/dt, which we reported in Fig. 1(b), is $\epsilon_2/|\epsilon|^2$ [up to a multiplicative factor, see formula (6)]. $\epsilon_2(q,\omega_{LO})$ represents the *density of states* of these carriers which can really emit the LO phonons of wave vector q. The dotted line represents the calculation without screening (i.e., $\epsilon=1$). The contribution of the two bands is included in the calculation of the total emission rate. The solid line is the full RPA calculation. Obviously, the emission of LO phonons, the wave vector of which is shorter than 1.25×10^6 cm^{-1}, is enhanced in the full RPA treatment. The impact in Raman-scattering exeriments may be very important, but the net effect on the total LO-phonon emission rate is expected to be small. This is already implicit from Fig. 1(b) because $d\langle E_\lambda\rangle/dt|_{LO}$ is proportional to the integral $\sum\int_0^{+\infty} q^2 dn_{LO}/dt|_\lambda dq$ [formula (7)], which represents the surface under the curves $q^2 dn_{LO}/dt$ which are very similar in the full RPA and no-screening approximations. As a result, we expect no important change in the total LO-phonon-emission rate calculated in the full RPA or without screening so long as the plasma density is lower than the critical density ρ_c previously defined.

The changes of $1/|\epsilon|^2$ and $\epsilon_2(q,\omega_{LO})/|\epsilon|^2$ at high density are reported in Figs. 2(a) and 2(b), i.e., when the plasma density becomes larger than the critical density $\rho_c=(4-7)\times 10^{17}$ cm^{-3}. First we chose to carry out the computations for the density $\rho=10^{18}$ cm^{-3}. The full RPA calculation of $1/|\epsilon|^2$ corresponds to the solid line 1 in Fig. 2(a). The dynamical resonance observed previously at lower density [Fig. 1(a), solid line 2] shrinks now because the LO-phonon energy $\hbar\omega_{LO}$ becomes smaller than the plasmon energy, so that $1/|\epsilon|^2$ tends to the static ap-

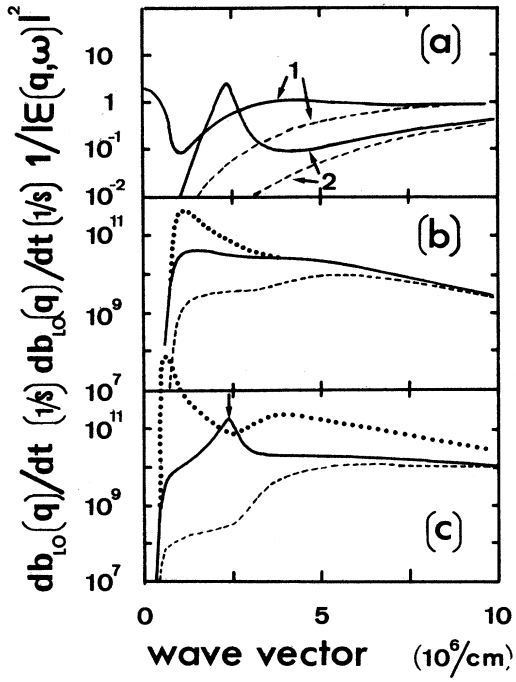

FIG. 2. Plasma temperature, 100 K; lattice temperature, 4 K. (a) Renormalization factor of the Frölich interaction. Curves 1: density $\rho=10^{18}$ cm^{-3}. Curves 2: density $\rho=10^{19}$ cm^{-3}. Solid lines, full RPA, dashed lines, static screening. (b) and (c) LO-phonon-emission rate. Solid lines, full RPA; dashed lines, static screening; dotted lines, no screening. (b) Density $\rho=10^{18}$ cm^{-3}. (c) Density $\rho=10^{19}$ cm^{-3}.

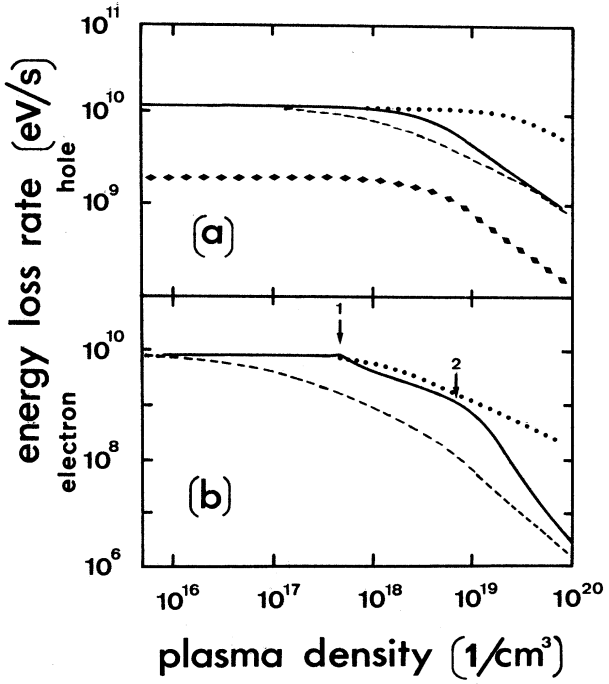

FIG. 3. Lattice temperature, 4 K. Solid line, full RPA; dashed line, static screening: dotted line, no screening. (a) Hole-energy-loss rate. The hole temperature is $T_v=100$ K, except for the diamond line which corresponds to $T_v=70$ K. (b) Electron-energy-loss rate. The electron temperature is 100 K.

proximation [dashed line 1 in Fig. 2(a)]. In Fig. 2(a), lines 2 correspond to the calculation of $1/|\epsilon|^2$ at the higher density $\rho=10^{19}$ cm^{-3}. As previously, the solid line is the full RPA calculation while the dashed line is the static one. Notice the antiscreening around $q\simeq 2.4\times 10^6$ cm^{-1} in the full RPA calculation due to the resonance of the LO phonons with the acoustical plasmons. The phonon-emission rates at the plasma densities of $\rho=10^{18}$ and 10^{19} cm^{-3} are reported, respectively, in Figs. 2(b) and 2(c). The solid lines are full RPA calculations. The dotted lines correspond to no screening ($\epsilon=1$) and the dashed ones to the static approximation. The enhanced emission which occurs in Fig. 2(c) around the wave vector $q\simeq 2.4\times 10^6$ cm^{-1} is always due to the resonance of LO phonons with *acoustical plasmons*. The two humps in the unscreened curve correspond to the density of states of electrons and holes which can emit the LO phonons. With respect to the low-density case of Fig. 1, the full dynamical calculations come close to the static screening. All these results, reported in Figs. 1 and 2, enable one to simply understand the dependence of the carrier-energy-loss rate as a function of the plasma density.

IV. NUMERICAL RESULTS: ENERGY-LOSS RATE

We plotted in Fig. 3(a) the hole-energy-loss rate at low temperature ($T_L=4.2$ K, $T_v=100$ K) as a function of the density.[35] In the full RPA screening (solid line), there is no change in the energy-loss rate up to the density $\rho\simeq 2\times 10^{18}$ cm^{-3}. In Fig. 3(b) is displayed the conduction-and energy-loss rate under the same conditions. There is a small enhancement of the electron-energy-loss rate around the density $\rho_c\simeq 4\times 10^{17}$ cm^{-3} due to the resonance of the LO phonon with the optical plasmon [arrow number 1 in Fig. 3(b)]. Note the great difference now between the results of the full RPA and the static approximation. The conclusion is that, in

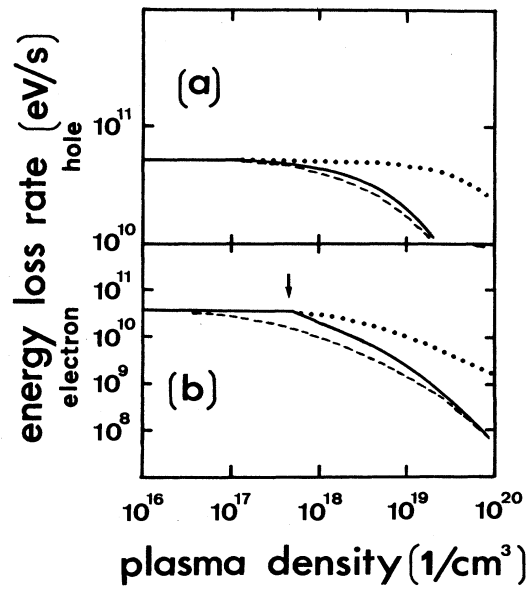

FIG. 5. Lattice temperature, 300 K. Solid line, full RPA; dashed line, static screening; dotted line, no screening. (a) Hole-energy-loss rate. The hole temperature is $T_v=350$ K. (b) Electron-energy-loss rate. The electron temperature is 350 K.

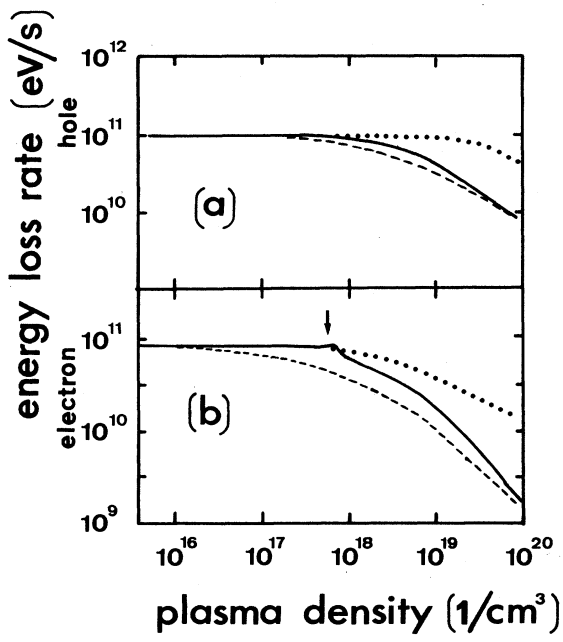

FIG. 4. Lattice temperature 4 K. Solid line, full RPA; dashed line, static screening; dotted line, no screening. (a) Hole-energy-loss rate. The hole temperature is $T_v=200$ K. (b) Electron-energy-loss rate. The electron temperature is 200 K.

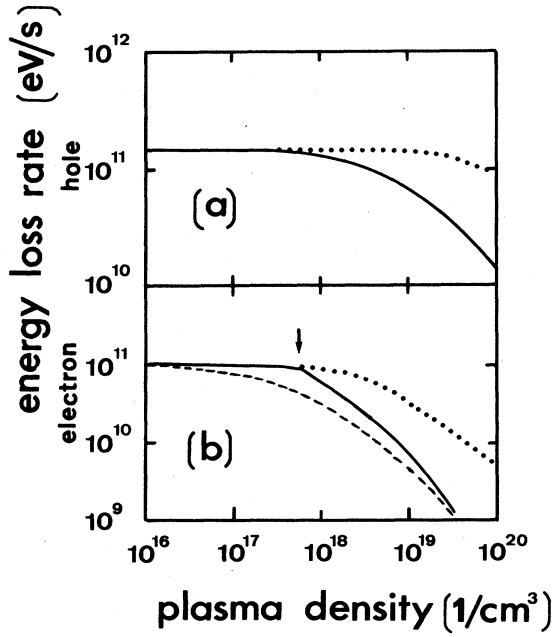

FIG. 6. Lattice temperature, 300 K. Solid line, full RPA; dashed line, static screening; dotted line, no screening. (a) Hole-energy-loss rate. The hole temperature is $T_v=450$ K. (b) Electron-energy-loss rate. The electron temperature is 450 K.

dynamical screening, the conduction-electron-loss rate is unchanged up to the density $\rho \simeq 5\times 10^{17}$ cm^{-3}. We must also stress that even at higher plasma densities, up to $\rho \simeq 10^{19}$ cm^{-3}, the dynamical screening leads to a correction factor of the order of 0.8 with respect to the simple and especially *convenient* "no-screening" model. The flat hump [arrow number 2 in Fig. 3(b)] is due to the resonance of LO phonons with the acoustical plasmons.

It is also of great interest to compare the hole-energy-loss rate to the electron one in cases of different electron and hole temperatures, for example, $T_h \simeq 70$ K and $T_c \simeq 100$ K. The diamond line in Fig. 3(a) just displays the hole-energy-loss rate at $T_h = 70$ K. By comparison with Fig. 3(b), we deduce that the electron-energy-loss rate is four times higher than that of the holes for densities ranging up to 5×10^{17} cm^{-3}. If the electron-hole thermalization is incomplete (i.e., $T_e > T_h$), as is concluded in many theoretical calculations,[19,21,36] the energy-loss rate due to LO-phonon emission by the electrons may become more important than the loss rate of the holes. This demonstrates the great impact of the dynamical screening as soon as a temperature difference appears between electrons and holes.

In Figs. 4, 5, and 6 are reported the energy-loss rates of the carriers at higher temperature, namely at 200, 350, and 450 K. In Figs. 4 and 5, the lattice temperature is 300 K. The results are very similar to the ones at 100 K and the same conclusions prevail. As a general rule, the energy-loss rate is unchanged up to the density $\rho \simeq (5-7)\times 10^{17}$ cm^{-3}, whatever may be the temperature. At high plasma density the acoustical-plasmon mode is strongly damped and even disappears. As a result, the transition to the static approximation for densities higher than 10^{18} cm^{-3} occurs faster than at low temperature.

V. CONCLUSION

We studied the renormalization of the polar-optical interactions in a high-density thermalized plasma. We used the full dynamical RPA to screen the Fröhlich interaction. It is concluded that up to the plasma density ρ_c defined by the relation $\hbar\omega_{\rm pl}(\rho_c) \simeq \hbar\omega_{\rm LO}$ [see formula (8)], there is no influence of screening on the carrier-energy-loss rate. For GaAs, $\rho_c \simeq (5-7)\times 10^{17}$ cm^{-3}. The absence of screening is in agreement with recent experimental works, especially heating effects.[26] At low temperature (say $T < 100$ K), because of the resonance of LO phonons with acoustical plasmons, the average screening of electrons in the conduction band is weak up to densities of the order of 10^{19} cm^{-3}. Plasma-dynamics calculations on the time scale 0.5–2 ps, which use the static screening of the PO interactions, must be revised.

ACKNOWLEDGMENTS

It is our pleasure to thank Professor P. Kocevar (Graz University) and Dr. W. Rühle (Max-Planck-Institut, Stuttgart) for several stimulating discussions and a critical reading of the manuscript.

APPENDIX: SCREENING OF THE ELECTRON-HOLE COLLISIONS

We prove in this appendix that, very generally, electron-hole collisions can be screened statically. Let us consider the following electron-hole scattering process: The electron is scattered from the wave vector $\mathbf{k}$ to the wave-vector $\mathbf{k}-\mathbf{q}$, and the hole from the wave vector $\mathbf{k}'$ to the wave vector $\mathbf{k}'+\mathbf{q}$. The energy ΔE exchanged in the process reads

$$\begin{aligned}\Delta E &= E_e(\mathbf{k}) - E_e(\mathbf{k}-\mathbf{q}) \\ &= E_h(\mathbf{k}') - E_h(\mathbf{k}'+\mathbf{q}) \\ &= \frac{\hbar^2}{m_e} qk\cos\theta - \frac{\hbar^2}{2m_e} q^2 \\ &= \frac{\hbar^2}{m_h} qk'\cos\theta' + \frac{\hbar^2}{2m_h} q^2 \ . \end{aligned} \tag{A1}$$

Here, θ (θ') is the angle between the vectors $\mathbf{k}$ and $\mathbf{q}$ ($\mathbf{k}'$ and $\mathbf{q}$). The main question in discussing screening in this process is, what are typically the wave vectors $\mathbf{k}$ and $\mathbf{k}'$ of an electron and a hole when a dynamical treatment of the dielectric function becomes necessary? For clarity let us begin with a numerical example, namely GaAs, at the density $\rho \simeq (5-7)\times 10^{17}$ cm^{-3} so that the plasmon energy is about 36 meV. The dielectric constant must be described dynamically if q is of the order of $(0.5-1)\times 10^6$ cm^{-1} and the energy exchanged of the order of the plasmon energy (see Fig. 2). Using $\Delta E \simeq 36$ meV and $q \simeq 10^6$ cm^{-1} in relation (A1) one obtains

$$k\cos\theta \geq 2.6\times 10^6 \text{ cm}^{-1} \ ,$$

$$k'\cos\theta' \geq 26\times 10^6 \text{ cm}^{-1} \ .$$

As a result, the kinetic energy of the electron and the hole involved in such a dynamical scattering must be high, namely

$$E_e \geq \frac{38}{\cos^2\theta} \gg 38 \text{ meV} \ ,$$

$$E_h \geq \frac{450}{\cos^2\theta'} \gg 450 \text{ meV} \ .$$

The hole must be very high in the valence band and, obviously, it is almost impossible to significantly populate a level of such high kinetic energy. It results that the static-screening approximation holds for the great majority of the electron-hole scatterings. We always obtain the same result when changing the plasma density chosen in our numerical example. So we conclude that, if the masses of the conduction band and valence band are very different, say m_c/m_v of the order of 5–10, statically screening the electron-hole collisions is an excellent approximation.

[1]R. Ulbrich, Phys. Rev. B **8**, 5719 (1973).
[2]E. O. Göbel and O. Hildebrand, Phys. Status Solidi B **88**, 645 (1978).
[3]J. Shah, Phys. (Paris) Colloq. **42**, C7-445 (1981).
[4]W. Graudszus and E. O. Göbel, Physica B+C **117/118B**, 555 (1983).
[5]T. Amand and J. H. Collet, J. Phys. Chem. Solids **46**, 1053 (1985).
[6]D. Bloch, J. Shah, and A. C. Gossard, Solid State Commun. **59**, 527 (1986).
[7]W. W. Rühle and H. J. Polland, Phys. Rev. B **36**, 1683 (1987).
[8]K. Leo and W. W. Rühle, Solid State Commun. **62**, 659 (1987).
[9]R. F. Leheny, J. Shah, C. V. Shank, and A Migus, Solid State Commun. **31**, 809 (1979).
[10]C. Minot, J. Chavignon, H. Le Person, and J. L. Oudar, Solid State Commun. **49**, 141 (1984).
[11]J. M. Wiesenfeld and A. J. Taylor, Phys. Rev. B **34**, 8740 (1986).
[12]J. L. Oudar, D. Hulin, A. Migus, A. Antonetti, and F. Alexandre, Phys. Rev. Lett. **55**, 2074 (1985).
[13]M. Pugnet, J. H. Collet, and A. Cornet, Solid State Commun. **38**, 531 (1981).
[14]J. H. Collet, M. Pugnet, A. Cornet, and T. Amand, Solid State Commun. **39**, 883 (1982).
[15]C. H. Yang and S. A. Lyon, Physica B+C **134B**, 309 (1985).
[16]J. R. Senna and S. Das Sharma, Solid State Commun. **64**, 1397 (1987).
[17]The description of the dynamics of the plasma-phonon system requires the resolution of transport equations very far from the thermodynamical equilibrium using numerical techniques (see, for example, Refs. 18 and 19). The consideration of dynamically screened interactions in athermal transport equations is an extremely difficult task, and in this respect, the problem of the quantitative description of the electron-hole plasma dynamics (plasma cooling, plasma expansion, quasiparticle energy renormalization, etc.) remains open.
[18]J. H. Collet and T. Amand, J. Phys. Chem. Solids **42**, 153 (1986).
[19]J. H. Collet, J. L. Oudar, and T. Amand, Phys. Rev. B **34**, 5443 (1986).
[20]W. Pötz and P. Kocevar, Phys. Rev. B **28**, 7040 (1983).
[21]M. Asche and O. G. Sarbei, Phys. Status Solidi B **126**, 607 (1984).
[22]A. C. Algarte, Phys. Rev. B **32**, 2388 (1985).
[23]M. Asche and O. G. Sarbei, Phys. Status Solidi B **141**, 487 (1987).
[24]P. Kocevar, in *Festkörperprobleme, Advances in Solid State Physics,* edited by P. Grosse (Vieweg, Braunschweig, 1987), Vol. 27, p. 197.
[25]E. J. Yoffa, Phys. Rev. B **23**, 1909 (1981).
[26]W. W. Rühle and H. J. Polland, Phys. Rev. B **36**, 1683 (1987).
[27]P. Kocevar (private communication).
[28]J. Kash and J. Tsang, Phys. Rev. Lett. **54**, 2151 (1985).
[29]M. Pugnet and J. H. Collet, Europhys. Lett. **7**, 567 (1988).
[30]It is important to stress that the quantum states to consider are different in the present problem of energy transfer from the electrons to the lattice than, for instance, in a Raman process. In a Raman process, photons are scattered by transitions of the full electron-phonon system. Here, on the contrary, the energy is transferred from the electrons to the lattice and we consider transitions of the isolated electron states. Otherwise, it would be impossible to distinguish which energy is lost by the electrons.
[31]Sh. M. Kogan, Fiz. Tverd. Tela (Leningrad) **42**, 474 (1962) [Sov. Phys.—Solid State **4**, 1813 (1963)].
[32]A. L. Fetter and J. D. Valecka, *Quantum Theory of the Many-Particle System* (McGraw-Hill, New York, 1971).
[33]In the usual semiconductors, the valence-band mass m_h is larger than the conduction-band one, m_c. So we deduce the following. (1) The approximation $[\mathrm{Im}(\Pi_c^{\mathrm{ir}})/|\epsilon(q,\omega)|^2]|1-\Pi_v^{\mathrm{ir}}|^2 \simeq \mathrm{Im}(\Pi_c^{\mathrm{ir}})/|\epsilon(q,\omega)|^2$ holds for the great majority of the LO-phonon emissions by the conduction electrons because $|1-\sum \Pi_v^{\mathrm{ir}}|^2$ may deviate from 1 only for q vectors which are not easily emitted by the conduction band. (2) $\Pi_c^{\mathrm{ir}}(q,\omega_{\mathrm{LO}})$ and $\Pi_v^{\mathrm{ir}}(q,\omega_{\mathrm{LO}})$ are very weakly overlapping functions so that $\mathrm{Im}(\Pi_v^{\mathrm{ir}})|\Pi_c^{\mathrm{ir}}(q,\omega_{\mathrm{LO}})/\epsilon(q,\omega_{\mathrm{LO}})|^2$ will contribute weakly in comparison to the quantity $\mathrm{Im}(\Pi_c^{\mathrm{ir}})/|\epsilon(q,\omega)|^2$.
[34]M. Costato and L. Reggiani, Phys. Status Solidi B **58**, 461 (1973).
[35]To compute the energy-loss rate, $db_{\mathrm{LO}}(q)/dt$ was typically calculated over the wave-vector interval $[0, 30\times 10^6\ \mathrm{cm}^{-1}]$.
[36]W. Pötz, Phys. Rev. B **36**, 5016 (1987).